

# Cerebellar Golgi cells in the rat: receptive fields and timing of responses to facial stimulation

Bart P. Vos, Antonia Volny-Luraghi, Erik De Schutter

Laboratory for Theoretical Neurobiology, Born-Bunge Foundation, University of Antwerp, Universiteitsplein 1, B2610 Antwerp, Belgium

**Keywords:** cerebellum, inhibitory interneurons, mossy fibre, parallel fibre, somatosensory system, trigeminal stimulation

## Abstract

Golgi cells are the only elements within the cerebellar cortex that inhibit granule cells. Despite their unique position there is little information on how Golgi cells respond to afferent input. We studied responses of Golgi cells to mechanical stimulation of the face, in Crus I-II of ketamine-xylazine anaesthetized rats. In 41 rats, 87 putative Golgi cells were identified, based on spike characteristics and on location of electrolytic lesions in the granular layer. They displayed a slow firing rhythm at rest (8.4 spikes/s). Most Golgi cells (84%) showed excitatory responses to tactile input. Their receptive fields (RFs) included, in 78%, the entire ipsilateral infraorbital nerve territory, and extended, in 14%, to other trigeminal nerve branches and, in 48%, to the contralateral face. Excitatory responses consisted of multiple, precisely timed ( $\pm 1$  ms) spikes. Most peristimulus time histograms (PSTHs) (69%) showed an early (5–10 ms) and a late (13–26 ms) excitatory component, with each component consisting of a single PSTH peak. In some PSTHs the early component was a double peak (<4 ms interval). In others, only one, early or late, PSTH peak was observed. The excitatory components were followed by a silent period (28–69 ms latency), the duration of which (13–200 ms) varied with response amplitude. In single cells, response profiles changed with stimulus location. In simultaneously recorded cells, evoked profiles differed for identical stimuli. Differences in RF size between early 'double' and 'single' peaks suggested that they resulted from direct mossy fibre and parallel fibre input, respectively. Late PSTH peaks were assumed to reflect corticopontine activation.

## Introduction

Before afferent information from mossy fibers impinges onto cerebellar Purkinje cells via the granule cell axons (Gundappa-Sulur *et al.*, 1999), it is preprocessed by local feed-forward and feed-back circuits, which are embedded in the granular layer of the cerebellar cortex (Eccles *et al.*, 1966b; Ito, 1984). The primary inhibitory neuron of this circuitry, the Golgi cell, may play an important role in this preprocessing. Golgi cells occupy a unique position, as they are the only neurons in the cerebellar cortex to receive both direct excitation (by mossy fibers) and indirect excitation (by parallel fibers). They are also the sole source of inhibition to granule cells. The latter observation led to the widely accepted theory (Marr, 1969; Albus, 1971; Ito, 1984) that Golgi cells perform a gain control function; Golgi cell inhibition is assumed to reset the threshold for granule cell firing so that the local granule cell activity remains within operational bounds. Feedback inhibition through the parallel fibre circuit seems well suited to perform such a gain control function, while the mossy fibre excitation could contribute by giving a 'look ahead' to future activity levels (Marr, 1969). Golgi cells are also unique in the vertebrate brain in that they are part of a pure feedback circuit; Golgi cells do not inhibit each other, nor do granule cells excite each other (Palay & Chan-Palay, 1974).

Most theories concerning the role of Golgi cells were inspired by descriptions of their anatomical connections. Spontaneous firing patterns of Golgi cells have been studied to some extent (Miles *et al.*, 1980; Van Kan *et al.*, 1993). Evoked responses of Golgi cells have been investigated in relation to vestibulo-ocular reflex adaptation (Miles *et al.*, 1980; Atkins *et al.*, 1997), locomotion (Edgley & Lidierth, 1987) or limb movement (Van Kan *et al.*, 1993). Reports on responses to natural, punctate stimuli are sparse (see Edgley & Lidierth, 1987). A recent study in which Golgi cells were selectively ablated in mice has shown that they are essential for normal cerebellar function (Watanabe *et al.*, 1998). The unique position of Golgi cells within the cerebellar circuitry, as well as predictions of our modelling studies (Maex & De Schutter, 1998a,b), led us to study the response properties of Golgi cells in greater detail (Vos *et al.*, 1999).

We describe the responses of Golgi cells in Crus I and II of the rat cerebellum to brief tactile stimulation of the face. The mossy fibre input, granule cell multiunit activity (Shambes *et al.*, 1978; Bower *et al.*, 1981; Welker, 1987; Bower & Kassel, 1990; Hartmann & Bower, 1998) and Purkinje cell responses (Bower & Woolston, 1983; Jaeger & Bower, 1994) to similar stimuli are well documented for this part of the rat cerebellum. We found that Golgi cells have unique response properties compared with other cerebellar elements; they have large receptive fields and show precisely timed responses to tactile stimulation. We postulate that the diversity of temporal response patterns observed in individual Golgi cells is the result of converging mossy fibre and parallel fibre inputs. Golgi cell responses

Correspondence: Dr B. P. Vos, as above.  
E-mail: bart@bbf.uia.ac.be

Received 9 December 1998, revised 11 March 1999, accepted 17 March 1999

were also characterized by a long silent period, the origin of which is unknown.

## Methods

### *Surgical preparation*

Thirty-eight male rats (300–450 g, 30 Sprague–Dawley and eight Wistar, IFFA CREDO, Brussels, Belgium) were anaesthetized with an i.p.-injected mixture of ketamine HCl (75 mg/kg; Ketalar, Parke–Davis, Warner Lambert Manufacturing Ltd, Dublin, Ireland) and xylazine HCl (3.9 mg/kg; Rompun, Bayer AG, Leverkusen, Germany) in normal saline (0.9% NaCl, Baxter nv, Lessine, Belgium). Supplemental doses (a third of the initial dose, injected i.m.) were given every 2 h to maintain anaesthesia. Three rats were anaesthetized with  $\alpha$ -chloralose (in 100% H<sub>2</sub>O, initial dose 50 mg/kg, followed by 37.5 mg/kg every 2 h, i.p.). Throughout the experiment heart rate was monitored (Hewlett-Packard 78342 A, Boeblingen, Germany) and toe-pinch reflexes were assessed to control the level of anaesthesia.

The rat's head was fixed in a Kopf stereotaxic frame (David Kopf Instruments, Bilaney Consultants GmbH, Düsseldorf, Germany) with unsharp earbars and a standard mouth piece with incisor bar. A homeothermic blanket system (Harvard Apparatus, South Natick, MA, USA) was used to maintain core temperature (37–38 °C). A midline incision was made and dorsal cranial muscles were removed to expose the caudal part of the skull and the first cervical vertebrae. Two stainless steel microscrews were implanted 3 mm caudal to bregma. The squamous part of the occipital bone was removed to expose Crus I and II of the cerebellum. All craniotomies were made on the left side. Before placement of the electrodes, the incisor bar was removed and the rat's head was tilted downward to level Crus II horizontally. The incisor bar was fixed on the implanted skull screws with dental cement (Hygenic Repair Resin, The Hygenic Corporation, Akron, Ohio, USA). The earbars were not removed. The dura was incised with the bent tip of a 29-gauge injection needle, reflected and removed. The cisterna magna was punctured and the cerebrospinal fluid drained to reduce cerebellar pulsation. The exposed cerebellar surface was covered with warm AGAR (2% in 0.1 M phosphate buffered saline).

### *Recording procedures*

Extracellular single unit recordings were made with sharp (1  $\mu$ m tip) tungsten microelectrodes (2 M $\Omega$ , World Precision Instruments, Stevenage, UK). Two or three electrodes were positioned simultaneously in Crus II (majority in Crus IIa) or Crus I (majority in Crus Ib and Ic) using Kopf micropositioners. Each electrode was lowered in the cerebellar cortex either vertically or in a slight angle (80°–90° from surface). If no spikes were isolated after a 2-mm descent, a new penetration was made. No attempts were made to map somatotopic organization. At the end of a recording session electrolytic lesions (cathodal, DC current, 15  $\mu$ A, 12 s; custom-built high-power source with timer; Grass constant current unit, Astro-Med Inc., West Warwick, RI, USA) were made to mark the location of the tip of each electrode. In some rats, the electrodes were then moved to a distinctly different part of Crus II or Crus I in search for new units.

Microelectrode signals were amplified and filtered (gain, 5000–15000; bandpass, 400–20 kHz), digitized and discriminated with a PC-controlled 'Multichannel Neuronal Acquisition Processor' (Plexon, Inc., Austin, Texas, USA). For discrimination of spike waveforms a real-time hardware-implemented combined time–voltage window discriminator (Nicollelis & Chapin, 1994) was used. Raw and discriminated signals were displayed on an oscilloscope

(BK Precision 2120, Maxtec International Corp., Chicago, IL, USA) and fed through an audio monitor (Grass AM8, Astro-Med Inc.) for further inspection. Waveforms and recorded spike trains (time series) were stored on computer disk for off-line analyses.

### *Identification of Golgi cells*

This study focused on the cerebellar Golgi cell population. Units encountered <0.4 mm below the cerebellar surface (molecular layer) were not considered (Eccles *et al.*, 1966b). Units that occasionally fired invariable, multispikes waveforms (complex spikes; Eccles *et al.*, 1966a; Thach, 1967; Llinás *et al.*, 1968) were identified as Purkinje cells. Units located at 0.3–0.4 mm from the cerebellar surface that fired large spikes at a high rate (interspike interval, ISI, <20 ms) were also categorized as Purkinje cells (simple spikes). For Purkinje cells, experimentation was limited to recordings of spontaneous activity after which the electrode was lowered in search for Golgi cells.

When passing the Purkinje cell layer, a sudden increase in background activity could be noticed; this increase of background noise was used as a landmark for entry in the granule cell layer (Miles *et al.*, 1980; Van Kan *et al.*, 1993). Putative Golgi cells were recognized by the distinctive rhythm of their spontaneous activity (Atkins *et al.*, 1997); their activity consisted of pronounced 'popping' of spikes, which rose well above the continuous background crackling, and which appeared at a rather slow cadence with appreciable intervals (no bursting).

Putative Golgi cells were quantitatively identified using criteria described by others (Eccles *et al.*, 1966b; Miles *et al.*, 1980; Edgley & Lidieth, 1987; Van Kan *et al.*, 1993; Atkins *et al.*, 1997): low discharge rates at rest (ISIs >20 ms); long-duration (>0.8 ms), diphasic (negative–positive or positive–negative) wave shapes; long tuning distances (electrode track distance, between the point at which spikes can be distinguished from background and a lower point at which the spike amplitude is maximal, of 50–150  $\mu$ m); no complex spikes; and location in the granular layer. During experiments, recording depth, waveform characteristics, firing rate and ISIs were continuously monitored to tentatively categorize units as Golgi cells. This categorization was further confirmed by additional quantitative analyses of spontaneous firing (see Results) and by histological proof that the electrolytic lesion marking the tip of the electrode was in the granule cell layer. Isolated units that did not meet the Golgi cell criteria, and which were not Purkinje cells, were categorized as mossy fibers or as unidentified units (see Results). Everywhere in the granular layer, small amplitude, short duration spikes could be recorded, but these spikes could not be isolated as single units. Therefore, they were considered to be granule cell spikes.

### *Physiological characterization*

Once an isolated unit was identified as a putative Golgi cell, spontaneous activity was recorded for at least two separate periods of at least 5 min each. Subsequently, mechanical taps with a hand-held cotton-tipped wooden rod were used to explore the facial receptive field (RF). In the first 19 rats, additional recordings of spontaneous activity were then made (see also Vos *et al.*, 1999). In the other 19 rats, somatosensory responses were quantitatively tested. In these experiments the rat's vibrissae were clipped to a length of 1 cm. A mechanical stimulation device driven by a Grass 11S digital stimulator (Astro-Med Inc.) was used to deliver controlled innocuous mechanical tap stimuli (10 ms) to (primarily) facial dermatomes. The custom-built mechanical stimulation device had a 1-mm diameter cylindrical stainless steel probe with flat surface (maximal excursion 2.5 mm) mounted on an electromagnetic activator (based on a 12-V

solenoid from Farnell Components, Maarssen, The Netherlands). The stimulator was fixed on a comparator stand with magnetic base (Mitutoyo, Brazil) to allow precise and stable positioning of the probe.

In five rats, the same location was stimulated at different frequencies (0.5–6 Hz). In three rats, mechanical stimulation was first applied to a vibrissa and the surrounding hairy skin (placement of the probe on the base of the vibrissa) and subsequently to the vibrissa alone (vibrissa glued to probe end). In 11 rats, the same stimulus (0.5 or 1 Hz) was applied to several (at least four) different facial loci on either side of the face. For each stimulus configuration the same stimulation paradigm consisting of  $\geq 100$  trials without stimulation, followed by  $\geq 100$  trials with stimulation was repeated at least twice (for example see Fig. 3, below).

### Data analysis

Off-line analyses of spike time series were made with STRANGER (Biographics, Inc., Winston-Salem, NC, USA) or MATLAB (The MathWorks, Inc., Natick MA, USA). For each unit, separate records of activity at rest were concatenated so that at least 3000 recorded spikes (per unit) were used for further analyses. From the concatenated records, the average firing rate (spikes/s) was calculated. ISI histograms (0.5–2-ms bins) were built, and CVs of the ISIs were calculated (SD ISI/mean ISI) to describe the regularity of the resting discharges quantitatively (Goldberg & Fernandez, 1971). In addition, a nonparametric equivalent of the CV (nCV) based on the median and the absolute deviation of the median (MAD) of the ISI was calculated (MAD ISI/median ISI) (see Results section).

Responses to mechanical stimulation were quantified as follows. For each unit, the mean firing rate (spikes/s) was determined over all stimulus trials for epochs of 30, 50 and 175 ms, before and after stimulus onset. To determine the response intensity, stimulus-evoked changes in firing rate were expressed as percentages [using the formula  $100 \times (\text{firing rate after} - \text{firing rate before}) / \text{firing rate before}$ ].

Rasterized traces with peristimulus spike trains, and peristimulus time histograms (PSTHs) were used to inspect evoked temporal spike patterns. In the majority of responses multiple peaks were observed on the PSTHs. Each peak results from the fact that, in most trials, a single spike occurred at a specific latency; the cumulative sum of spike counts per bin per peak would then be  $\leq N$  (number of trials). To quantify the latency, accuracy and robustness of the temporal spike patterns, fine resolution PSTHs (0–250 ms poststimulus; 0.25 ms bin width) were constructed. A critical value representing background activity (counts per bin) was determined, based on the firing rate during the trials without stimulation (50 ms epochs), as the 95% confidence limit of the 'spontaneous' counts per bin [mean counts per bin +  $2.96 \times$  standard error of the mean (SEM)]. The putative beginning of a peak was defined as the first bin with a spike count more than this critical value. The end of a peak was defined as the last bin before five consecutive bins with counts below the critical value (gap of 1.25 ms). If no gaps occurred, the end of a peak was defined as the bin at which the cumulative spike count (starting from the first bin) reached 97.5% of  $N$ . Peaks for which the total number of bins was  $> 20$ , or in which the cumulative spike count was  $< 10\% N$ , were not considered significant. The cumulative spike count within a peak was expressed as a percentage of  $N$  to assess the robustness of each peak.

Each peak was subsequently fitted with a Gaussian curve (custom-developed MATLAB function; average fraction of variance unexplained was  $0.19 \pm 0.06$ ); the mean and standard deviation (SD) of

the fitted Gaussian distributions determined the latency and accuracy of the peak, respectively.

To quantify the robustness of the entire PSTH profile, the average ratio of the percentage of trials that contributed a spike to the peak, to the SD (width) of the peaks, was calculated over all peaks, as:  $\sum_i \{[(\text{cumulative sum of spikes in peak}/N) \times 100] / \text{SD}_i\} / n$ , where  $N$  is the number of stimulus trials,  $n$  the number of PSTH peaks,  $i$  the peak number and  $\text{SD}_i$  is the SD of the corresponding fitted Gaussian distribution.

### Statistical analysis

Factorial analysis of variance with *post hoc* comparisons according to Fisher's protected least square difference (PLSD) was used to compare physiological characteristics of different cell categories, and timing characteristics and response intensities of different response profiles. Paired Student *t*-tests were used to compare the pre- and poststimulation firing rates of the same cell. A  $\chi^2$ -test of independence was applied to assess differences in frequencies of observed response profiles between stimulus locations within the same cell, or between cells for the same stimulus location. A nonparametric analysis of variance by ranks (Friedman's test) was used to test differences in RF size (in arbitrary units) for different response profiles (see Results). Correlations were tested with Spearman's rank correlation coefficient (Spearman's  $\rho$ ).

### Histology

At the end of the experiment, rats received a lethal dose of sodium pentobarbital (120 mg/kg i.p.; Nembutal, SANOFI, Libourne, France). The brain was removed and fixed in 4% formalin. The cerebellum was embedded in paraffin and 10- $\mu\text{m}$  transverse or sagittal sections were cut and stained with cresyl violet to visualize the electrolytic lesions. Sections with lesions were photographed and drawn with a camera lucida. Camera lucida drawings were scanned (AGFA Studiostar, AGFA-Gevaert, Mortsel, Belgium) and retraced (Adobe Illustrator, Adobe Systems Inc., San Jose, CA, USA) to produce the line drawings in this paper. As only one unit was isolated per electrode track, the location of each of the recorded units could be reconstructed.

### Ethical considerations

Animals were treated and cared for according to the ethical standards and the guidelines for the use of animals in research of the National (USA) Research Committee on Pain and Distress in Laboratory Animals (N.R.C. 1992). Testing procedures were approved by the Ethical Committee of the University of Antwerp, in accordance with Federal Laws.

## Results

### Identification of the recorded units

In 38 ketamine-xylazine anaesthetized rats, stable recordings were obtained from 171 units. Based on the presence of complex spikes, 18 units were positively identified as Purkinje cells. Another 20 units were classified as Purkinje cells firing simple spikes; their action potentials were large and had a long duration ( $> 0.8$  ms), they had high firing rates with relatively short but variable ISIs (Table 1) and the electrolytic lesions were at the border between the molecular and the granular layer.

For 87 units that also fired large, long-duration action potentials consisting of negative-positive wave shapes, the electrolytic lesion was positioned within the granule cell layer (e.g. Fig. 1). These units

TABLE 1. Firing characteristics of recorded units at rest

Cell Type	( <i>n</i> )	Spike width (ms)	Firing rate (spikes/s)	Median ISI (ms)	CV of ISI (SD/mean)	nCV of ISI (MAD/median)
Purkinje cells SS	38	1.04 (0.94–1.37)	27.9 (4.03–81.4)*	17 (5–109)*	2.65 (0.41–5.72)*	0.47 (0.15–0.73)
Purkinje cells CS	18	1.34 (0.21–4.73)*	1.34 (0.21–4.73)*	114 (42–608)	1.13 (0.49–2.16)	0.66 (0.46–0.82)
Golgi cells (ketamine-xylazine)	87	1.15 (0.87–1.85)	8.42 (1.89–18.1)	97.24 (31–223)	0.92 (0.19–2.36)	0.43 (0.13–0.70)
Golgi cells ( $\alpha$ -chloralose)	5	1.22 (1.10–1.46)	3.19 (0.59–6.37)	560 (127–1444)*	0.92 (0.57–1.51)	0.48 (0.33–0.76)
Mossy fibers	30	0.65 (0.31–0.72)*	8.57 (1.21–24.9)	100 (4–1406)	1.55 (0.82–4.29)*	0.71 (0.51–0.92)*
Unidentified Units	16	0.64 (0.54–0.77)*	13.9 (1.44–31.1)*	91 (4–798)	1.41 (0.49–4.29)*	0.64 (0.21–0.92)*

Data are given as means, with ranges in parentheses. \* $P < 0.001$ , Fisher's PLSD, significant differences from Golgi cells recorded in ketamine-xylazine anaesthetized rats.

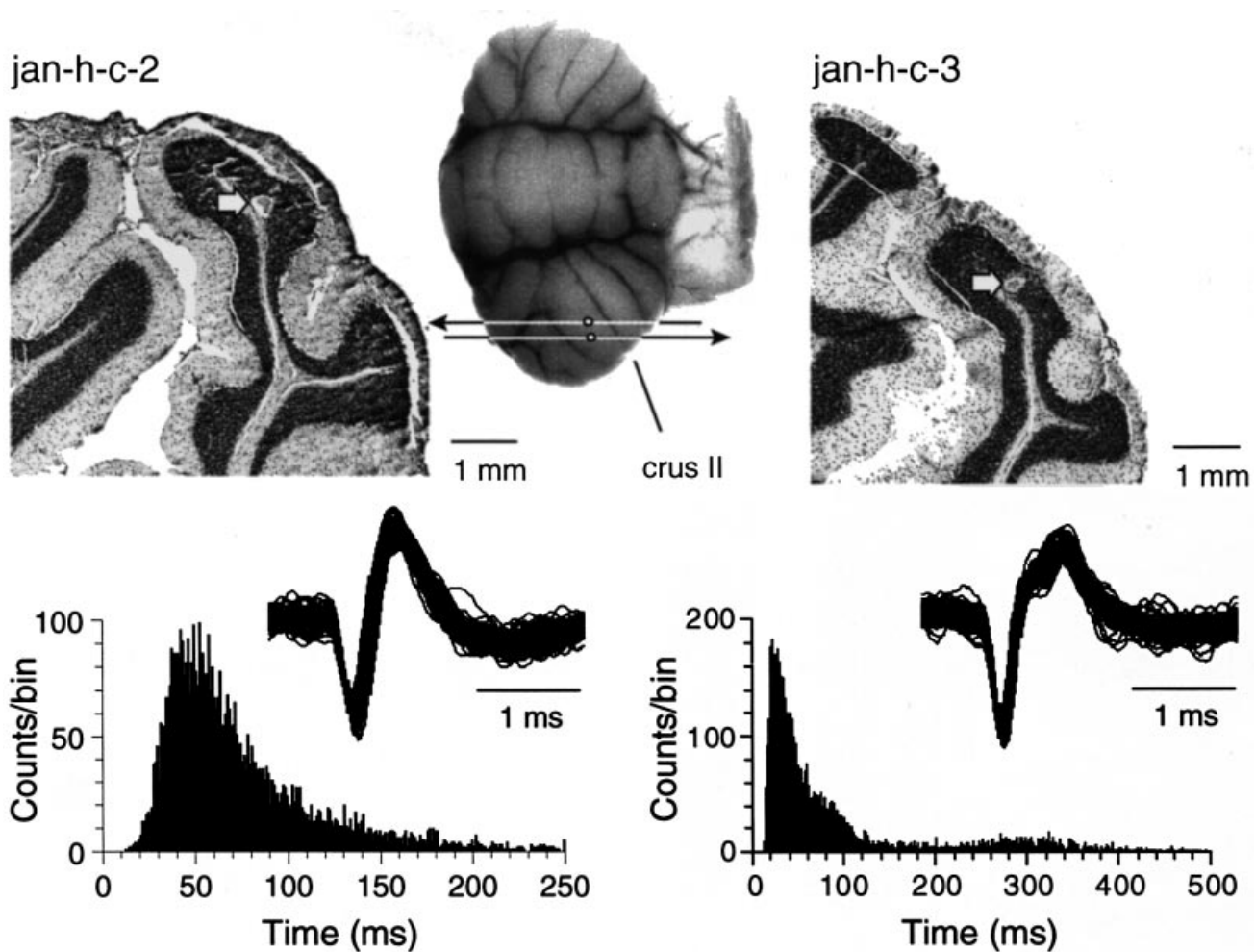


FIG. 1. Examples of units identified as Golgi cells based on location of the electrolytic lesion, waveform and firing pattern. Top part shows photomicrographs with the position of electrode penetrations (middle) and the location of the electrolytic lesions (fat white arrows) on two parasagittal sections (10  $\mu$ m, cresyl violet stain) through Crus II. Superimposed records of 100 recorded waveforms of each unit are shown in the middle. Bottom part shows the respective ISI histograms (respectively 1 ms and 2 ms bins) based on 5360 spikes (jan-h-c-2) and 4603 spikes (jan-h-c-3) captured during a 400-s recording of activity at rest. Average firing rates of the cells were, respectively, 13.4 and 11.4 spikes/s. Median ISIs were 62 ms and 42 ms, and nCVs were 0.43 and 0.54.

had long tuning distances (electrode movements of  $> 100 \mu$ m) and did not show complex spikes. Based on their position and wave shape characteristics these units were classified as putative Golgi cells (Table 1, Fig. 2). Golgi cells were also recognized by their slow, fairly regular (not bursting) firing rhythm (see further). The average yield of Golgi units was about two per rat; in 40% of the rats only one Golgi

cell could be isolated, in 60% a pair of Golgi cells was recorded simultaneously, and in 20% simultaneous recordings of three Golgi cells were realized.

Thirty units fired short, small-amplitude action potentials ( $< 0.8$  ms). They were difficult to isolate and had very short tuning distances. When the electrode was moved, they would typically

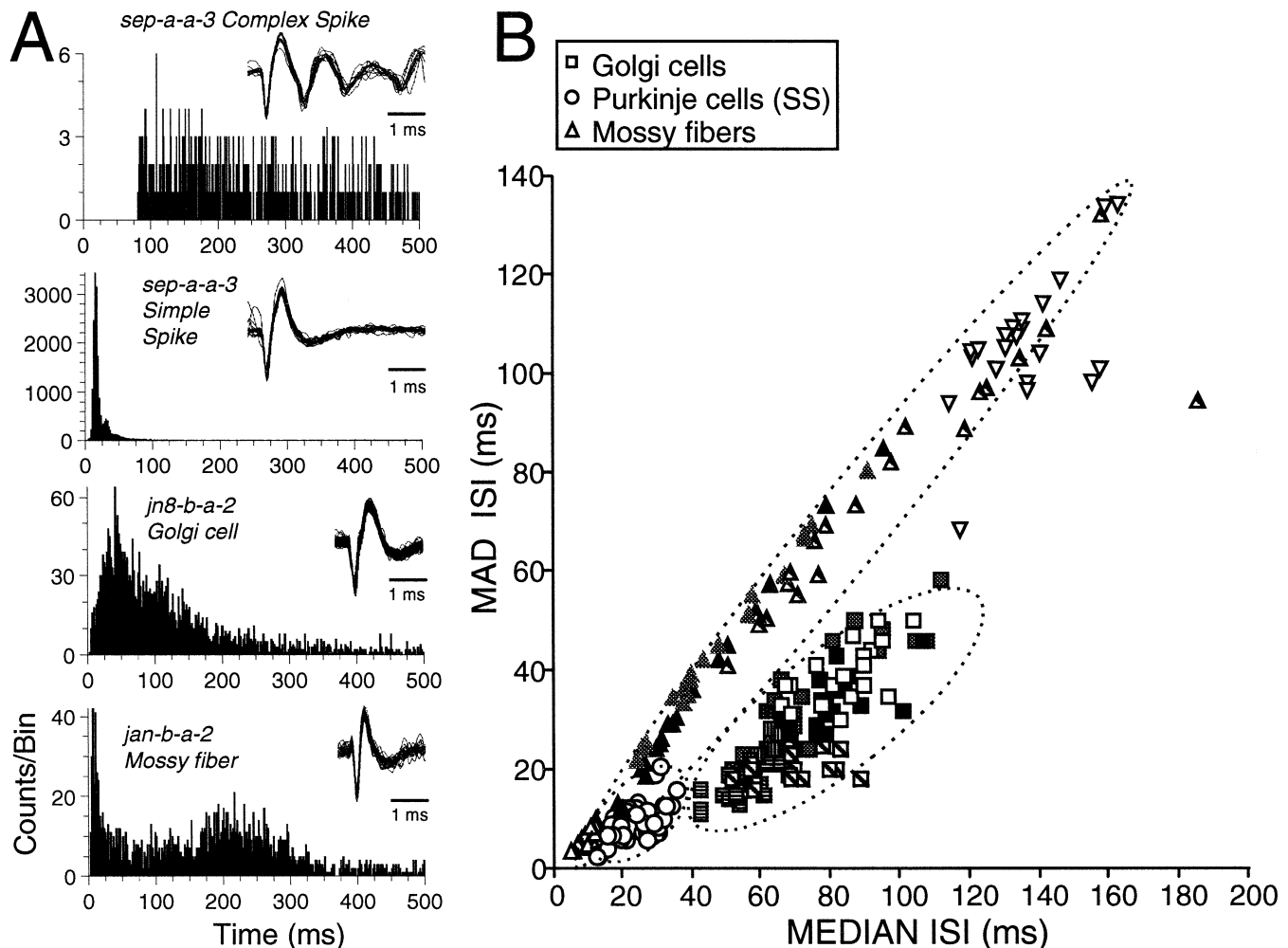


FIG. 2. Identification of recorded units based on characteristics of activity at rest. (A) Superimposed records and ISI histograms (2 ms bins) of complex and simple spikes (SS) recorded from a Purkinje cell (*sep-a-a-3*, 1000-s trial), spikes recorded from a Golgi cell (*jn8-b-a-2*, 440-s trial) and from a mossy fibre (*jan-b-a-2*, 460-s trial). Respective firing rates were 1.2 (complex spikes), 18.5 (simple spikes), 6.6 (Golgi cells) and 4.2 (mossy fibre) spikes/s. (B) Relation between median ISI and MAD of the ISI. Based on recorded spike trains, the median and MAD of the ISI were computed for 20 samples of 100 consecutive ISIs (total of 2000 spikes) from each unit. In the graph, data from five different cells (different shadings), representative of each group are plotted (squares, Golgi cells; circles, simple spikes of Purkinje cells; triangles, mossy fibres).

disappear without showing high-frequency injury discharges, like those that were often observed in units identified as arising from Golgi cells. The spontaneous activity of the short action potentials was characterized by the presence of bursts (triplets or quadruplets of spikes, interval < 5 ms) which occurred rhythmically. Consequently, their ISI histograms showed two distinct peaks (see Fig. 2A, unit *jan-b-a-2*). In five cases there was a close temporal relationship between these bursts and spontaneous rhythmic facial muscle twitches. These muscle twitches, which produced vibrissal movements, were not related to the depth of anaesthesia; noxious pinch to hind paws or tail did not evoke a withdrawal response or a change in the heart rate. We classified 26 of these units as mossy fibres because the electrolytic lesions marking the electrode positions were located in the white matter close to the granular layer. Another four units that showed short duration wave forms and similar bursting behaviour at rest, but for which the electrolytic lesion was located in the granular layer, were also categorized as putative mossy fibres (Table 1).

Sixteen units had very short action potentials, they did not show bursting activity and were located in the granular layer. They were classified as unidentified units.

In the three  $\alpha$ -chloralose-anaesthetized rats, five units were identified as Golgi cells. They showed lower firing frequencies at rest (Table 1), but their response characteristics were not different from those recorded in ketamine-xylazine-anaesthetized rats (Table 1, other results not shown).

#### *Golgi cell firing characteristics at rest*

Units characterized as Golgi cells were tonically active at rest and had a typical firing rhythm without bursts (see Methods). Their average firing rates and median ISIs (Table 1) were well within the ranges reported by others for Golgi cells in anaesthetized rodents (Schulman & Bloom, 1981), awake rabbits (Atkins *et al.*, 1997), anaesthetized (Van Kan *et al.*, 1993), decerebrate (Eccles *et al.*, 1966b) or awake cats (Edgley & Lidieth, 1987), or awake primates (Miles *et al.*, 1980; Van Kan *et al.*, 1993).

The typical firing rhythm has been described as highly regular (Miles *et al.*, 1980; Schulman & Bloom, 1981), or as slower and more regular than that of Purkinje cell simple spikes (Edgley & Lidieth, 1987) or mossy fibre discharges (Van Kan *et al.*, 1993).

TABLE 2. Extent and laterality of Golgi cell RFs

	Frequency		Laterality of Golgi cell RFs		
	Without RFs	With RFs	RF ipsilateral only	RF includes contralateral parts	Total
	<i>n</i> (%)	<i>n</i> (%)	<i>n</i> (%)	<i>n</i> (%)	<i>n</i> (%)
All Golgi cells	14 (16)	73 (84)			87 (100)
Golgi cells with RFs					
Restricted*			6 (8)	0 (0)	6 (8)
Territory of one Vth-nerve branch			25 (34)	32 (44)	57 (78)
Greater than one Vth-nerve branch			7 (10)	3 (4)	10 (14)
Totals with RFs			38 (52)	35 (48)	73 (100)

Data are given as numbers of cells, with percentages in parentheses. \*Equivalent to area between four vibrissae.

Eccles *et al.* (1966b), however, appraised the Golgi cell firing pattern as 'rather irregular' and Atkins *et al.* (1997) did not find evidence for a regular pattern either.

The ISI distributions of Golgi units were unimodal with a broad peak with an average median of 97.24 ms (Table 1), indicating low firing rates and a fairly irregular firing pattern (Figs 1 and 2). In addition, most Golgi cell ISI distributions were asymmetrical with a long tail caused by the frequent appearance of long (>200 ms) ISIs (e.g. Fig. 1, unit jan-h-c-3). Golgi cells did not show spontaneous bursting as reflected by the absence of ISIs >10 ms. As shown in Fig. 2A and Table 1, Purkinje cells fired simple spikes at a significantly higher rate, while putative mossy fibers showed typical bimodal ISI distributions resulting from the presence of triplets or quadruplets of spikes fired with intervals smaller than 5 ms. Granule cell spikes could not be isolated as single units.

The mean CVs of the ISIs of each of the different neuronal classes (Table 1) were considerably higher than in other studies (e.g. Miles *et al.*, 1980; Atkins *et al.*, 1997). This is probably due to the considerably longer recording trials (see Methods) used in this investigation compared with the cited studies. Also, all ISI distributions clearly deviated from the normal Gaussian distribution. We therefore opted to use the nonparametric equivalents of the SD and the mean to calculate a 'nonparametric' CV (nCV; Table 1). Based on this nCV, Golgi cell firing at rest appeared no more regular than simple spike firing of Purkinje cells, but it was more regular than the bursting firing pattern of presumed mossy fibers.

A similar differentiation could be made when, for 20 consecutive samples of 100 ISIs taken from the recorded spontaneous activity of individual units, the spread (MAD) of the median ISIs was plotted against their median (Fig. 2B). It appeared that most data points of one unit were positioned on a straight line through zero, the slope of which equalled the nCV. Separate data points of individual neurons of the same class could be grouped in distinct clusters (Fig. 2B). This figure shows that the ratio of the MAD and the median of the ISIs remained fairly stable, although in Golgi cells and presumed mossy fibers, different samples of 100 ISIs showed considerable variations in the respective values. These shifts were most striking for the presumed mossy fibre units.

#### Receptive field properties

The RFs of 48 Golgi cells (10 singles, 16 pairs, two trios) were explored using hand-held mechanical stimuli; in 39 Golgi cells (three singles, nine pairs, six trios) responses to controlled mechanical stimuli (see Methods) were quantitatively studied. Table 2 summarizes the observed frequencies of cells for which a RF was found, and the extent of these RFs. The majority of recorded Golgi cells (73 out of 87, 84%) showed a strong

'excitatory' response (i.e. increase in activity) to brief innocuous mechanical stimulation (Figs 3–5). The localization of the RFs of the recorded Golgi cells was in concordance with previously described trigeminal projections to Crura I and II (Welker, 1987). Golgi cell RFs were much larger than expected from described fractured somatotopic maps in these cerebellar lobules (e.g. Bower *et al.*, 1981; Welker, 1987; Bower & Kassel, 1990). In 57 out of 73 (78%) Golgi cells with a RF, the RF covered the entire territory of the maxillary branch of the trigeminal nerve [rhinarium, all rows of vibrissal pad and upper lip (Waite & Tracey, 1995)]. In 10 out of 73 (14%) Golgi cells the RF extended to parts of the territories of the ophthalmic (e.g. cornea) or mandibular (e.g. lower lip, tongue) branches of the trigeminal nerve (e.g. Fig. 4). In addition, in almost half of the Golgi cells (35 out of 73) the RF included parts of the contralateral facial dermatomes. Because of their large RFs, Golgi cells located in the same lobule had overlapping RFs (see e.g. Figs 3 and 5).

#### Timing of evoked spikes

The use of controlled mechanical stimuli allowed a detailed quantitative analysis of the temporal characteristics of responses of 39 Golgi cells recorded in 19 rats. PSTHs were constructed based on at least 100 trials per stimulus configuration.

First inspection of these PSTHs revealed that Golgi cell responses consisted of multiple spikes, the timing of which showed a distinct, rather precise temporal pattern (Fig. 3); multiple narrow peaks could be discerned on the PSTHs. Each peak represents the fact that in a substantial number of stimulus trials, a single spike occurred at a specific, fixed latency after stimulus onset. Also, individual Golgi cells appeared capable of responding to different stimulus configurations with different temporal spike patterns (Fig. 4). In order to investigate the temporal patterns, PSTH peaks were quantitatively defined and fitted with a Gaussian curve (see Methods). A first statistical analysis was based on a sample of 85 PSTHs, consisting of one of each of the different temporal patterns produced by each of the 39 Golgi cells. The temporal pattern of two responses was considered different if the number of significant peaks (see Methods) on the PSTH differed, or if, in case of an equal number of PSTH peaks, their latencies differed significantly (no overlap of 95% confidence intervals of latencies: mean  $\pm$  2.97  $\times$  SEM).

The majority of evoked responses (59 out of 85, 69%) showed both an early (5–10 ms) and a late (13–26 ms) peak on the PSTH (Figs 3–5). In 13 of these, an additional delayed peak was observed at 34–49 ms. Observed latencies of the three response components were consistent with latencies to mechanical facial stimulation observed in the granular layer or in Purkinje cells

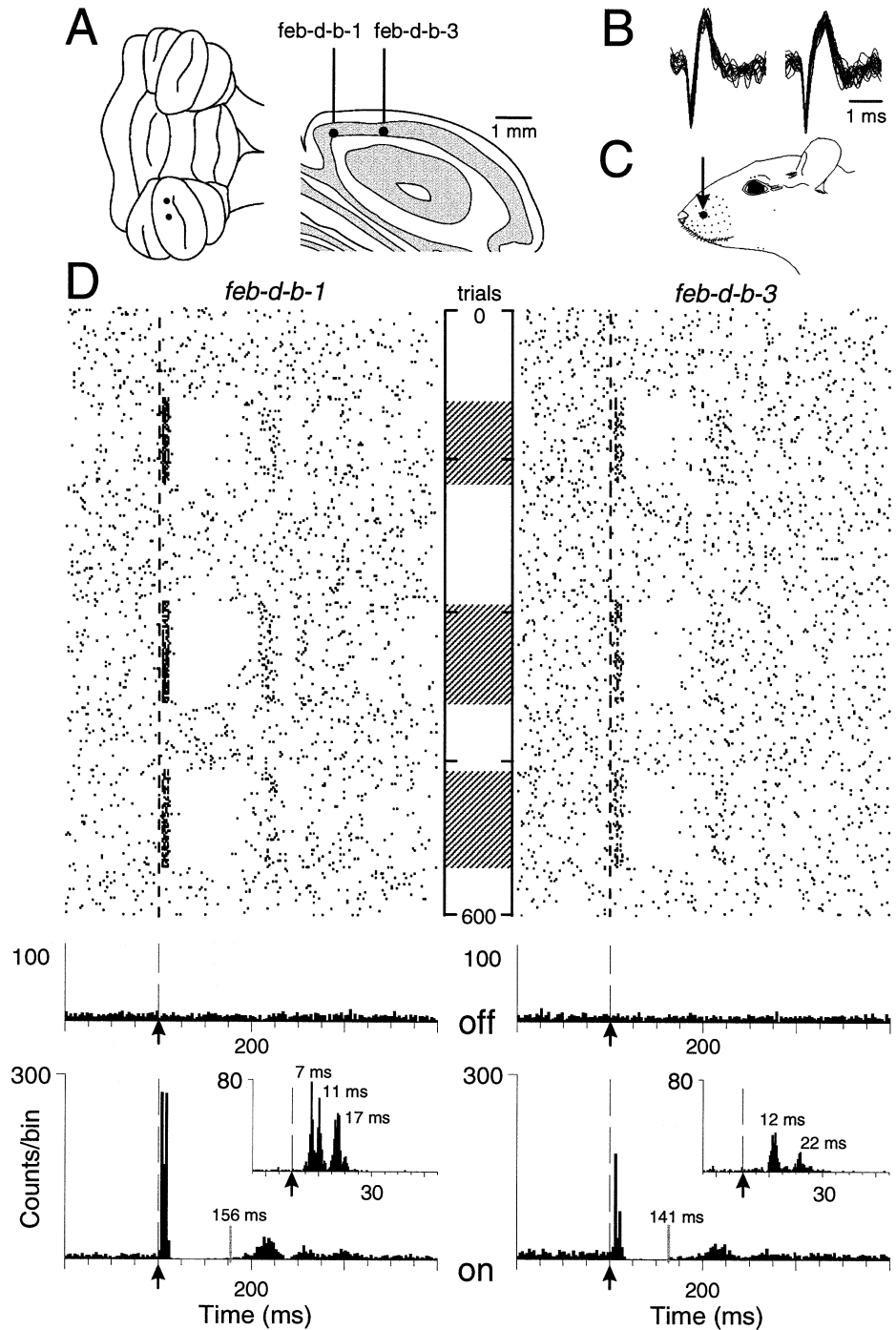


FIG. 3. Example of stimulation-evoked responses in two Golgi cells. (A) Schematic representation of the position of the electrodes in Crus IIa and line drawing of the transverse section with the location of the electrolytic lesions in the granular layer. (B) Superimposed records of 100 spikes from each unit. (C) The hairy skin bounded by vibrissae B3, B4, C3 and C4 was mechanically stimulated at 1 Hz (1 mm probe, 10 ms duration). (D) For each unit, rasterized traces of recorded spikes captured on 600 successive trials are shown (from 200 ms before, to 600 ms after, stimulus onset, indicated by dashed line); hatched bars between rasters indicate three periods, respectively, 88, 102 and 96 successive trials with stimulation. The lower panels show per-event histograms for each unit (low resolution from 200 ms before, to 600 ms after, stimulus onset, 2 ms bins; high resolution from 15 ms before, to 55 ms after, stimulus onset, 0.5 ms bins; arrows indicate stimulus onset) with the total number of spikes per bin over 286 trials with stimulation. Firing rates at rest (30 ms epoch before stimulation) were 3.6 (feb-d-b-1) and 7.3 (feb-d-b-3) spikes/s. Post stimulus firing rates were 79.2 and 36.2 spikes/s (30 ms epoch). The spike pattern evoked by the same stimulus is different in both simultaneously recorded units. Unit feb-d-b-1 fires at almost all stimulus presentations with the same spike pattern. Both units show a silent period which ends with a rebound increase in activity (end of silent period is indicated).

(Bower *et al.*, 1981; Bower & Woolston, 1983; Welker, 1987; Morissette & Bower, 1996).

Based on the number of PSTH peaks and their latencies, four response profiles were differentiated (Fig. 6): (i) those consisting only of an early single peak (latency <13 ms) and no late component (13 out of 85; 'Single/-' in Fig. 6A, C and D); (ii) those consisting only of a late single peak and no early component (13 out of 85; '-/Single' in Fig. 6A, C and D); (iii) those with an early component consisting of two (or three, e.g. Fig. 4) closely spaced peaks (interval <4 ms) of nearly equal amplitude (termed 'early double peak') and a single peak as the late component (18 out of 85; 'Double/Single' in Fig. 6A, C and D); and (iv) those with a single peak as early and late component

(41 out of 85; 'Single/Single' in Fig. 6 A,C and D). As demonstrated in Fig. 6B and C, the first spikes of responses that showed an early double peak (Double/Single) systematically had the shortest latencies. The early component of the Double/Single profiles was also significantly more precise (average SD over both peaks; Fig. 6D) and reproducible (expressed as the percentage of trials contributing a spike to the PSTH peak; average over both peaks; Fig. 6E) compared with early single peaks of Single/Single profiles. No such differences were found between the late components of Double/Single and Single/Single profiles. Note also that for responses consisting of two or more components, the precision and robustness of the later peaks gradually diminished (Fig. 6D and E). Finally, the latencies of responses consisting of

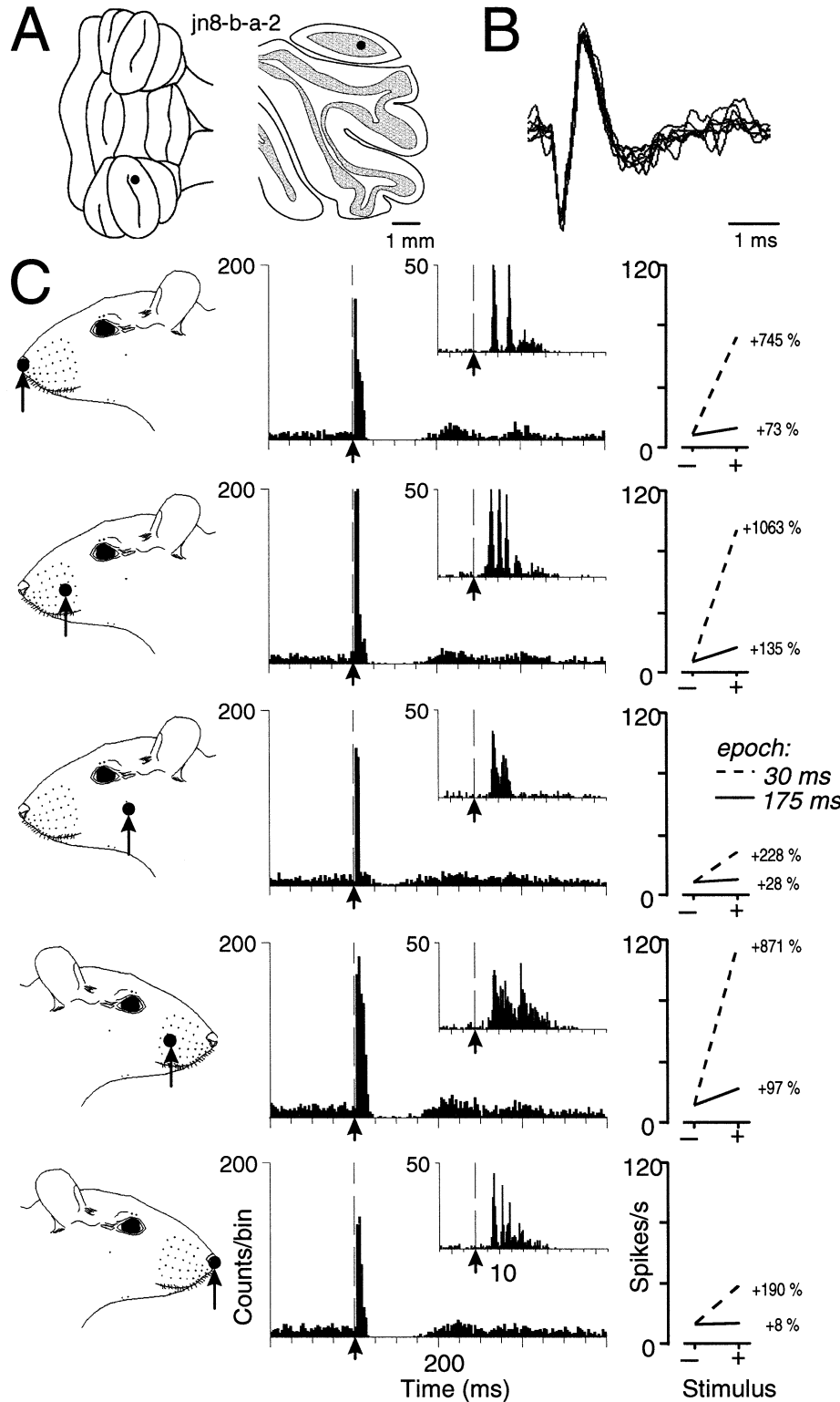


FIG. 4. Large RFs of Golgi cells. (A) Schematic representation of the position of the electrode in Crus IIa and line drawing of the transverse section with the location of the electrolytic lesion in the granular layer. (B). Superimposed records of 100 spikes. (C) The same stimulus (1 mm probe, 10 ms duration, 0.5 Hz) was applied to five different areas (dots). Middle panels show respective PSTHs (low resolution from 200 ms before, to 600 ms after, stimulus onset, 2 ms bins; high resolution from 15 ms before, to 55 ms after, stimulus onset, 0.5 ms bins; arrows indicate stimulus onset) with the total number of spikes per bin over 200 trials per stimulated area. Right panels are line graphs representing firing rates before (-) and after (+) stimulation based on 30 ms (dashed line) and 175 ms (full line) peristimulus epochs. The percentage increases in firing rate are indicated. Large responses were evoked for each stimulus location, but the response pattern varied.

an early single peak only (Single-), were on average longer, showed a greater variability and were less robust (Fig. 6C-E)

The average ratio of the percentage of trials that contributed a spike to the peak, to the SD (width) of the peak, over all peaks was used as a measure of the robustness of the complete temporal spike pattern (see Methods). Responses with the shortest latencies (mostly profiles with an early double peak) appeared most robust

(Fig. 7A). Over all cells, a Spearman's rank correlation coefficient of  $-0.501$  was found ( $P < 0.001$ ). Similarly, a positive correlation ( $+0.564$ ,  $P < 0.0001$ ) was found between the intensity of the response (firing rate in the first 50 ms poststimulus epoch) and the robustness of the temporal pattern; the more intense the response, the more precise was the timing of the evoked spikes (Fig. 7B).

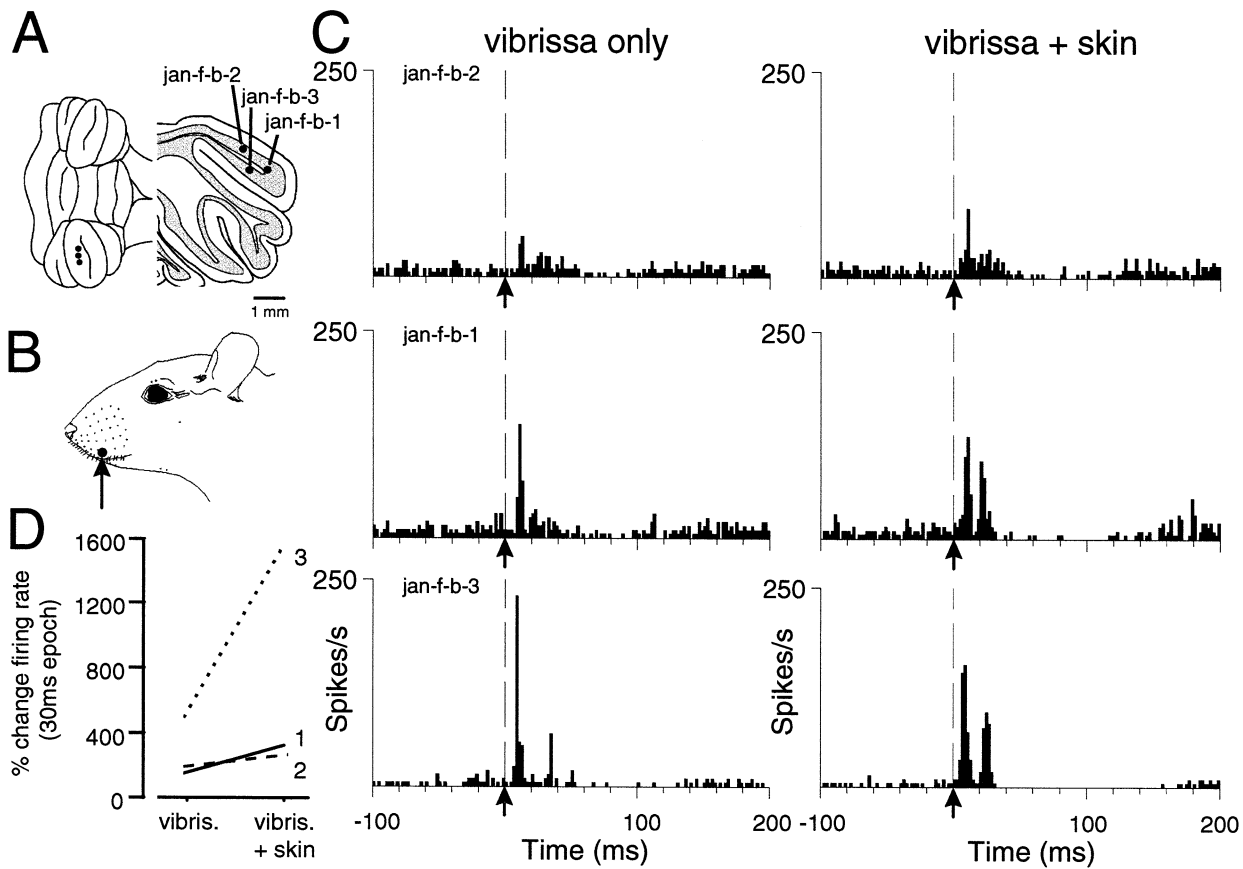


FIG. 5. Effect of number of afferents activated on Golgi cell responses. (A) Schematic representation of the position of the three electrode penetrations in Crus IIa and line drawing of the transverse section with the location of the electrolytic lesions in the granular layer. (B) The same stimulus (1 Hz, 1 mm probe, 10 ms) was applied to vibrissa E3 alone or to the hairy skin surrounding it. (C) PSTHs (from 100 ms before, to 200 ms after, stimulus onset; 2 ms bins) with the responses (spikes/s) to each stimulus (102 and 306 trials, respectively) of the three units. (D) Line graph representing the percentage increase in firing rate (30 ms epochs) evoked by each of the stimuli in each of the units. While all units responded more to the more intense stimulus, the temporal pattern of the spike response was only changed in the third unit.

#### Golgi cell responses include a long silent period

On average, Golgi cells quadrupled their firing rate in the first 30 ms after stimulus onset (from 8.4 to 47.5 spikes/s; +466%; see Figs 4–6 and 8A). When larger poststimulus epochs (175 ms) were considered, changes in firing rate were smaller, though still significant (from 8.17 to 12.34 spikes/s; +51%; Figs 4 and 9A). This effect reflected the presence of a long silent period in the responses of the majority (33 out of 39) of the units tested. The silent period had a latency of 28–69 ms (average, 45 ms) and a duration of 13–200 ms (average, 93 ms). Its presence was independent of the type of anaesthesia used (results not shown). The duration of the silence correlated (Spearman's  $\rho=0.646$ ,  $P=0.0002$ ) with the intensity of the response (discharge rate in 30 ms epoch; Fig. 8B). This relation was not only found between different cells, but also within cells (Figs 5 and 8B). In some responses discharge rates increased again at the end of the silent period (Figs 3 and 4).

#### Timing of spikes varies with stimulus location and cell localization

The typical examples shown in Figs 3–6 illustrate that individual Golgi cells produced different temporal spike patterns in response to different stimulus configurations, and that one particular stimulus was capable of evoking different temporal spike patterns in different,

though simultaneously recorded Golgi cells. In order to explore which factors determined the temporal characteristics of the evoked response profiles, three stimulus parameters were varied.

In three rats, responses of eight Golgi cells (one pair and two trios) to stimulation of a single vibrissal hair were compared with responses to stimulation of the hairy skin surrounding that vibrissa. It was assumed that stimulation of the vibrissa alone activated a smaller number of trigeminal afferents than stimulation of both the vibrissa and the surrounding hairy skin (Sharp *et al.*, 1988). In all instances increasing the stimulus intensity did affect the intensity of the response (average 86% increase in percentage change in firing rate, e.g. Fig. 5D). In only one Golgi cell, stimulation of the hairy skin produced a different temporal spike pattern from stimulation of the corresponding vibrissa alone (Fig. 5, unit jan-f-b-3).

In five rats (11 Golgi cells: four pairs and one trio) the frequency of the mechanical stimulus was varied (at least three different frequencies). Neither the intensity nor the timing of the evoked response were affected by changes in stimulus frequency within the range used (0.5–6 Hz).

In 11 rats, responses of 17 Golgi cells (four pairs, three trios) to stimulation of three to nine different locations of the face were recorded. Only one cell showed the same spike pattern for each of the three different loci that were stimulated. Figure 9A

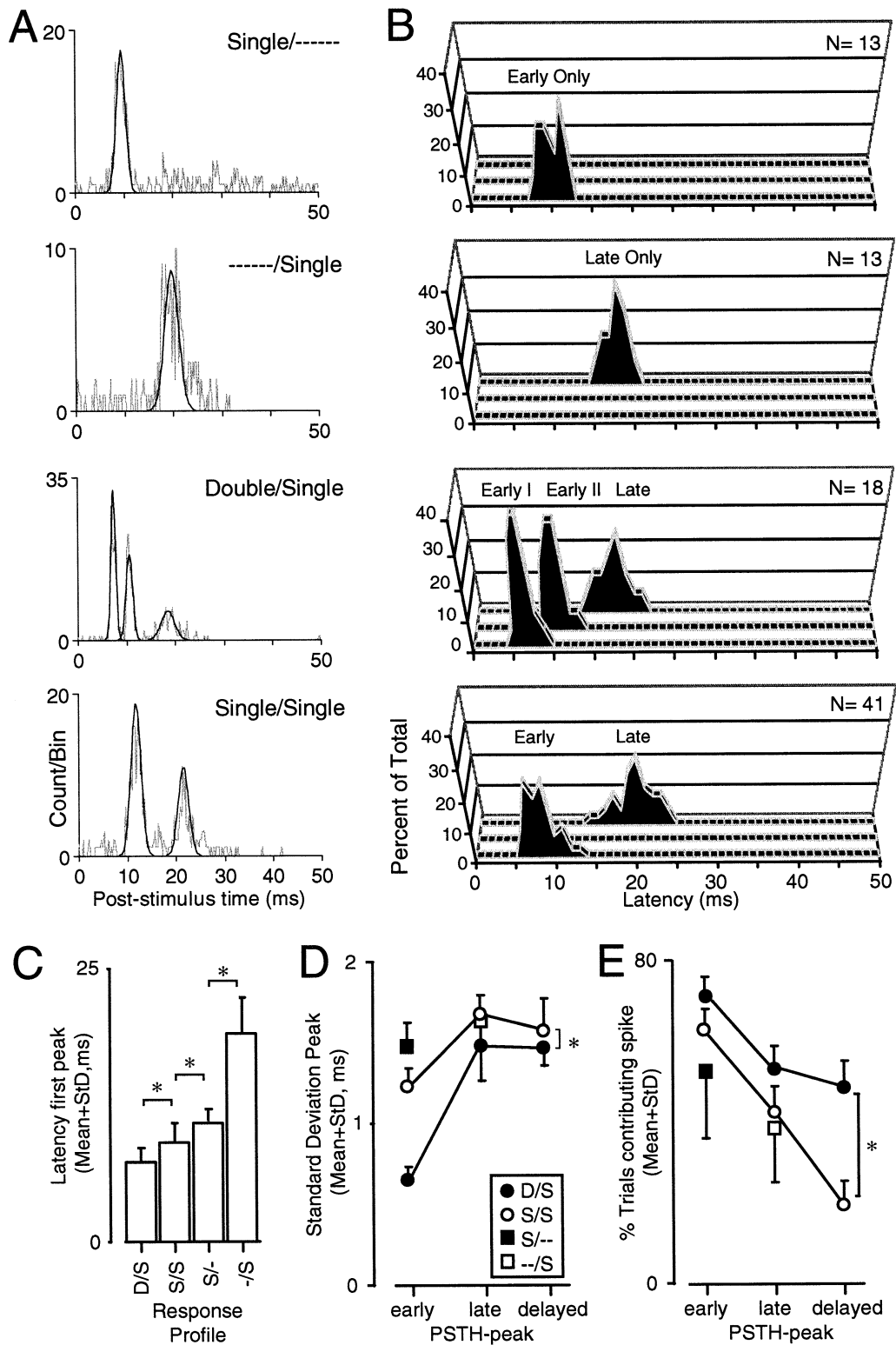


FIG. 6. Response patterns observed in cerebellar Golgi cells. (A) PSTHs (0–50 ms, 0.25 ms bin width) with Gaussian fits of each of the peaks, representing typical examples of each of the four different response profiles. (B) Frequency distribution of the latencies of the early and late component for each response profile (1 ms bin, counts are expressed as percentage of total; total number of responses, *N*, on which each histogram is based is indicated). Data on the delayed component are not shown (C) Bar chart indicating the mean latency of the first peak for each of the four response profiles (respective *N*-values are the same as in B). Asterisks indicate significant differences (not all shown, Fishers' PLSD,  $P < 0.001$ ). (D and E) Line graphs indicating, respectively, the accuracy (SD of PSTH peak) and robustness (percentage of trials contributing spike to peak) of the early, late and delayed components in each of the response profiles. Asterisks indicate significant differences between groups (ANOVA,  $P < 0.05$ ).

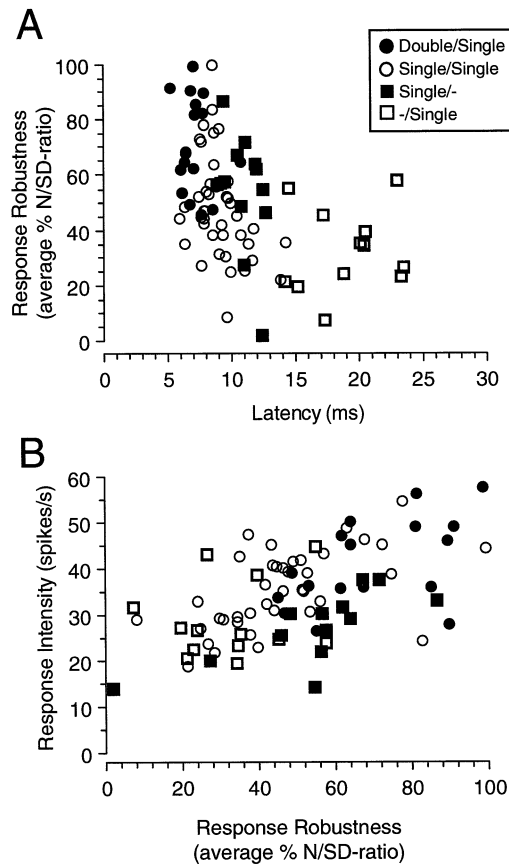


FIG. 7. Robustness of the spike pattern is related to the latency and intensity of the response. The robustness of the complete spike pattern was determined as the average ratio of the percentage of trials that contributed a spike to the peak to the SD (width) of the peak, calculated over all peaks in the PSTH (see Methods). (A) Scatterplot illustrating that the more robust responses (Y-axis) had the shorter latencies (X-axis) (Spearman's  $\rho = -0.501$ ,  $P < 0.001$ ). Note also that these responses had an early double PSTH peak (filled circles). (B) Scatterplot illustrating that the more robust the complete spike pattern was (X-axis), the more intense the response (spikes/s in 50 ms poststimulus epoch) (Spearman's  $\rho = 0.564$ ,  $P < 0.0001$ ).

demonstrates that 16 out of 17 Golgi cells produced different temporal spike patterns in response to stimulation of at least half of the different locations.

Most of the simultaneously recorded Golgi cells had overlapping RFs; in many rats, stimulation of a particular location evoked responses in all (two or three) simultaneously recorded Golgi units (Figs 3 and 5). Identical temporal spike patterns were evoked in only two out of 13 pairs of simultaneously recorded cells in response to stimulation of each of the stimulated loci. In four out of 13 pairs the temporal spike pattern was different for more than half of the stimulated loci. In six out of 13 pairs, stimulation of each of the loci resulted in a different temporal spike pattern.

#### Receptive fields with an 'early double peak' response component are restricted

One strategy to gain insight into the origin of the afferent pathways that contribute spikes to each of the different PSTH peaks consists of plotting, per cell, the RF of each of the PSTH components (early double, early single and late single peak). Figure 9B shows, for two cells, the RFs of each of the three components, delineated as areas on

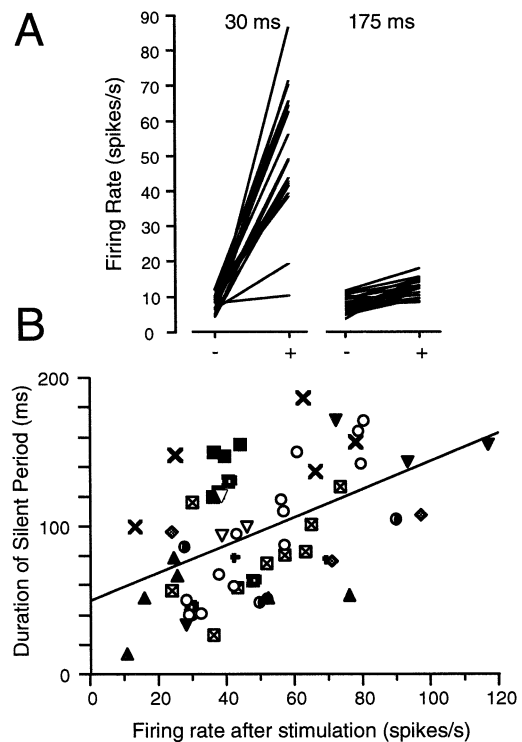


FIG. 8. Most Golgi cell responses show a 'silent' period. (A) Firing rate (spikes/s) before (-) and after (+) stimulation determined in 30 ms or 175 ms epochs from stimulus onset. For each of the Golgi cells data from the facial stimulus configuration (at least 100 trials) that yielded the strongest response are plotted. (B) Scatterplot showing the relation between response strength (X-axis; firing rate during 30 ms poststimulus epoch) and the duration (in ms) of the silent period (Y-axis). Different symbols represent data of different units, with responses to each stimulus (different area, frequency or intensity); at least 100 trials) plotted separately. Both between and within units, the duration of the silent period is correlated to the strength of the initial response.

a schematic drawing of the rat's face. PSTH profiles with an early double peak (D/S) were evoked from restricted facial areas, while those showing an early single peak (S/S) covered large parts of the rat's face on both sides. The largest RFs were observed for the second component (latency  $> 13$  ms). This was confirmed by statistical analysis; in each of 17 cells each of the components was given a rank based on the arbitrary size of their respective RFs (1, smallest; 3, largest). The mean rank of the early double peak component (over all cells) was significantly lower than that of the two other components (mean ranks: early double, 1.417; early single, 2.208; late single, 2.375.  $P < 0.05$ , Friedman's test).

## Discussion

Although Golgi cells play an important role in the cerebellar cortex (Watanabe *et al.*, 1998), systematic studies of their responses to punctate stimulation are sparse. We found that responses to brief tactile stimuli showed complex and accurate temporal characteristics which make Golgi cells unique compared with other cerebellar neurons.

#### Technical considerations

It should be acknowledged that all evidence for identifying recorded units as Golgi cells was circumstantial. We used the same criteria for Golgi cell identification as used by others (see Results). For all units

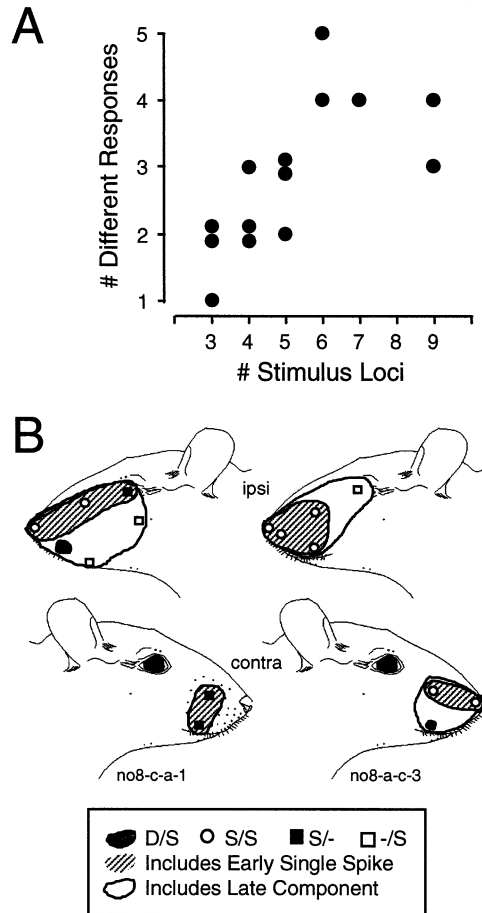


FIG. 9. Receptive field statistics and distributions. (A) Scatterplot of the number of different stimulus locations tested, and the number of different response profiles observed, for each individual cell ( $N=17$ ). (B) Illustration of the relation between the RFs and spike timing. For two typical cells, the RFs of early double PSTH peak (black area), the early single PSTH peak (shaded area), and the late component (white area) are drawn on graphical representations of the rat's face, ipsi- and contralateral to the recording site (above and below, respectively). In addition, the exact location from which each of the response profiles were evoked, are indicated by symbols.

classified as Golgi cells, electrolytic lesions were located within the granular layer. All putative Golgi cells fired large, long-duration action potentials, which had considerable tuning distances and remained well isolated throughout the entire recording session (sometimes >6 h), despite nearby placement of other electrodes, or a long series of mechanical stimuli. These observations are consistent with a large unit of origin. It is known that Golgi cells are the largest neural element in the granular layer (Palay & Chan-Palay, 1974). We are confident that none of the identified Golgi cells were granule cells. The cell bodies of granule cells are very small and they constitute such a tightly packed, dense mass (Ito, 1984) that isolating one granule cell spike without capturing waveforms produced by neighbouring granule cells is impossible with the metal electrodes of the type used in the present study.

The anaesthetic used, and its route of administration (i.p.), did not allow for a perfect control of the level of anaesthesia. However, the recorded waveforms, like the spontaneous firing rates, remained practically unchanged throughout the long recording sessions. Moreover, identical anaesthetic regimes have often been used (e.g. Bower *et al.*, 1981; Morissette & Bower,

1996). In addition, spontaneous firing rates for each of the neuronal classes observed in the present study were well within those reported by others. Finally, we did not find Golgi cell response characteristics to be changed when a different anaesthetic was used. An advantage of anaesthetized preparations compared with awake animals is the better stimulus control and the higher yield of Golgi cell recordings per rat.

#### Firing properties of Golgi cells

Spontaneous firing rates were similar to those observed for Golgi cells in other preparations. Golgi cells recorded in this study did not fire very regularly, similar to those of Eccles *et al.* (1966b) and Atkins *et al.* (1997). Golgi cells did not burst as mossy fibre units did. The identification of mossy fibre units was based on their typical dual peaked ISI distribution and the location of most of these units in the white matter. Because of their typical ISI these units could not be confused with Purkinje cell axons (Fig. 2A), while their high firing rate also excluded climbing fibers.

We attempted to quantify the 'typical' firing rhythm (see Results) by calculating a nonparametric CV, nCV, which allowed Golgi cells to be distinguished reliably from other cerebellar units (Fig. 2B). This objective measure can be used to identify units in future studies.

#### Response properties of Golgi cells

The majority of recorded Golgi cells in Crus I and Crus II responded to tactile stimulation and had facial somatosensory RFs. This is consistent with the fact that both granule cells and Purkinje cells in these cerebellar lobules have been reported to respond to stimulation of trigeminal areas (e.g. Shambes *et al.*, 1978; Bower *et al.*, 1981).

In contrast to the mosaic of small RFs found for field potentials in the granule cell layer (Bower *et al.*, 1981; Shambes *et al.*, 1978) or Purkinje cells (Bower & Woolston, 1983), most Golgi cells in Crus I and II had rather large RFs. In the present study, the majority of Golgi cell RFs covered at least the entire territory of the infraorbital nerve [maxillary branch of the trigeminal nerve: vibrissal pad, rhinarium and upper lip (Waite & Tracey, 1995)] ipsilateral to the recording site. Sometimes the RF extended to the territories of the ophthalmic or mandibular nerve, and it often included parts of the contralateral face. It should be acknowledged that RF testing was primarily confined to facial dermatomes, so that the presence of discontinuous RFs that included parts of limbs or trunk could have been missed.

Large RFs have also been reported for Golgi cells recorded by others. Edgley & Lidieth (1987) found that 85 out of 87 Golgi cells responded to tactile stimulation in the awake cat; the majority had large and bilateral RFs. Also in halothane-anaesthetized rats, an unspecified proportion of Golgi cells responded to peripheral stimulation (Schulman & Bloom, 1981). In barbiturate-anaesthetized monkeys only few Golgi cells (three out of 18) responded to somatosensory stimulation (Van Kan *et al.*, 1993). In awake monkeys however, all of the Golgi cells tested (five out of five) responded to passive joint manipulation, though they lacked directional specificity (Van Kan *et al.*, 1993). For Golgi cells recorded in the cerebellar flocculus of the awake rabbit and the awake monkey, a great diversity of modulation patterns was found (Miles *et al.*, 1980; Atkins *et al.*, 1997). The latter two findings are, like the presence of large tactile RFs observed by others and in the present study, an indication of an enormous convergence of excitatory inputs onto single Golgi cells.

We also found that Golgi cells responded to tactile stimulation with precisely timed temporal spike patterns. In some cases responses were highly robust, with close to 100% of trials firing a spike within a 1-ms window (Fig. 7A). In most responses an early and a late

component could be discerned. Based on the nature of the early component and the absence of either one of the two components, we described four different response profiles. Individual Golgi cells were capable of producing different response profiles (e.g. Fig. 4). Stimulus location and cell localization appeared related to the temporal characteristics of the evoked responses. Conversely, stimulus amplitude or frequency could affect the response amplitude, but had little effect on its temporal pattern.

#### *Possible trigeminal afferent pathways to Golgi cells*

There are two possible afferent pathways that convey trigeminal input to cerebellar Golgi cells. First are the trigeminocerebellar projections by second order neurons in the trigeminal nuclear complex of the brainstem (Darian-Smith & Phillips, 1964; Watson & Switzer, 1978; Woolston *et al.*, 1982; Huerta *et al.*, 1983). In addition, in rat, first order trigeminal afferents were also found to project directly to the cerebellar cortex (Jacquin *et al.*, 1982). Second are the corticopontine projections (Bower *et al.*, 1981; Morissette & Bower, 1996). Both arrive in the cerebellar cortex as mossy fibers.

The latencies of the early ( $8.9 \pm 1.7$  ms) and late ( $19.1 \pm 3.6$  ms) excitatory components of Golgi cell responses corresponded closely to the latencies described for the early and late component of granular layer field potential responses (8–10 ms and 16–22 ms, respectively) which were recorded in Crus II under similar experimental conditions (Morissette & Bower, 1996). This strongly suggests that the early and late excitatory components of the Golgi cell responses were caused by mossy fibre input via trigeminocerebellar and corticopontine projections, respectively. Morissette & Bower (1996) also showed that the corticopontine projections (which caused the late response component) had a larger projection zone in the granular layer. We found similarly that the late component had the largest RF. In addition, the late component was not as robust or as accurate as the early component. A longer pathway, involving multiple synapses is expected to transmit input less faithfully.

#### *Golgi cell responses reflect excitation by both mossy and parallel fibers*

It is not very likely that the whole of each response was caused by direct mossy fibre input to the Golgi cell. Mossy fibre input to Crus I and II of the rat cerebellum is fractured, consisting of many patches, each of which receives tactile input from only a small part of the rat's face (Shambes *et al.*, 1978; Bower *et al.*, 1981; Bower & Kassel, 1990). The trigeminal and corticopontine mossy fibre RFs largely overlap (Bower *et al.*, 1981; Morissette & Bower, 1996). Consequently, pure mossy fibre excitation of a Golgi cell should result in a small RF corresponding to one or, at most, a few patches (see Welker, 1987 for review). In contrast, Golgi cells had very large RFs.

The extensive RFs probably reflected an important excitation by parallel fibers, which because of their length (Pichitpornchai *et al.*, 1994) can originate in many different patches and, as such, carry input from parts of the rat's face different from the mossy fibre projection field. Some patches in Crus II have contralateral or bilateral RFs (Welker, 1987); this could explain the bilateral Golgi cell RFs we observed in 41% of the cells.

Nevertheless, several of our observations suggest that the early double peak found in a substantial proportion of Golgi cell response profiles resulted from direct mossy fibre input, while the early single peaks were probably produced by parallel fibre excitation. Responses with an early double peak had significantly shorter delays and a significantly higher spike timing accuracy (i.e. less jitter). Moreover,

'early double peak' response components were more intense and had a more restricted RF than other response components. All these observations suggest that the early double peak component reflects a strong mossy fibre excitation. The early single peak components had much larger RFs, a longer delay and were less accurately timed. Therefore we hypothesize that single peak components were primarily the result of parallel fibre excitation that was delayed and less precise in timing because of the slow and variable parallel fibre conduction velocities (Bernard & Axelrad, 1991; Vranesic *et al.*, 1994). It should be stressed that PSTH profiles with and without an early double peak were sometimes observed in the same individual Golgi cell. This rules out the possibility that all early double peak responses were recorded directly from mossy fibers (and not from Golgi cells).

In view of the fact that responses with only one component also had large RFs, it is possible that they reflect a purely parallel fibre evoked event: either only the trigeminocerebellar input (only early component) or only the corticopontine input (only late component). This observation is consistent with the assumption that the transmission over the parallel fibers weakens with increasing distance from the original mossy fibre input.

#### *Significance of the long silent period*

Almost all Golgi cell responses included a silent period. This silent period was quite noticeable because the cells were spontaneously active before the stimulus. Silent periods have been observed in evoked activity of presumed Golgi cells in anaesthetized cats, in response to parallel and mossy fibre stimulation but not in response to inferior olive stimulation (Eccles *et al.*, 1966b), in awake cats in response to peripheral stimulation (Armstrong & Rawson, 1979) and in anaesthetized rats in response to inferior olive stimulation (Schulman & Bloom, 1981). They have also been observed in other parts of the somatosensory system, including the pontine nuclei (Mihailoff *et al.*, 1992) and the ventral posterior nucleus of the thalamus (Nicollelis & Chapin, 1994).

The cause and function of the silent period remain unclear. While the presence of similar silent periods in other somatosensory pathways suggests that a lack of mossy fibre activation contributed to the silent period, it is likely that endogenous properties of the cerebellar circuit also play a role. The latter is supported by the strong correlation between the magnitude of Golgi cell responses and the subsequent silent period. The strong tonic component of granule cell inhibition that was recently described in cerebellar slice preparations (Brickley *et al.*, 1996; Wall & Usowicz, 1997) may contribute to the silent period. As this tonic inhibition is postulated to be caused by Golgi cell activity, resulting in spillover of GABA which activates high affinity receptors (Rossi & Hamann, 1998), it should be correlated with the amplitude of Golgi cell responses. Such tonic inhibition of granule cells will cause an interruption of parallel fibre excitation to the Golgi cell, enhancing the effect of diminished or absent mossy fibre input. Supporting evidence for this scenario is the strong on-beam inhibition evoked by short bursts of parallel fibre excitation in an isolated guinea pig cerebellum preparation (Cohen & Yarom, 1998).

In conclusion, neither the large RFs nor the fine temporal pattern of Golgi cell responses to tactile stimulation, including the silent period, are predicted by theories of cerebellar function that assume a pure gain control function of Golgi cells (Marr, 1969; Albus, 1971). Our results may necessitate a re-evaluation of the role of Golgi cells in cerebellar function (Maex & De Schutter, 1998b).

## Acknowledgements

The authors wish to thank Inge Bats for the photography, and Evelyne De Leenheir and Ursula Lubke for the histology. We gratefully acknowledge the technical wizardry of Mike Wijnants and thank Reinoud Maex for constructive criticism of earlier versions of the manuscript. This research was funded by HSFPO (RG87/94), by IPA Belgium (P4/22) and by the Fund for Scientific Research–Flanders (FWO-VI) (number 1.5.504.98). B.P.V. and E.D.S. are supported by the FWO-VI.

## References

- Albus, J.S. (1971) A theory of cerebellar function. *Math. Biosci.*, **10**, 25–61.
- Armstrong, D.M. & Rawson, J.A. (1979) Activity patterns of cerebellar cortical neurones and climbing fibre afferents in the awake cat. *J. Physiol. (Lond.)*, **289**, 425–448.
- Atkins, M.J., Van Alphen, A.M. & Simpson, J.I. (1997) Characteristics of putative Golgi cells in the rabbit cerebellar flocculus. *Soc. Neurosci. Abstr.*, **23**, 1287.
- Bernard, C. & Axelrad, H. (1991) Propagation of parallel fiber volleys in the cerebellar cortex: a computer simulation. *Brain Res.*, **565**, 195–208.
- Bower, J.M., Beerman, D.H., Gibson, J.M., Shambes, G.M. & Welker, W. (1981) Principles of organization of a cerebro-cerebellar circuit. Micromapping the projections from cerebral (SI) to cerebellar (granule cell layer) tactile areas of rats. *Brain Behav. Evol.*, **18**, 1–18.
- Bower, J.M. & Kassel, J. (1990) Variability in tactile projection patterns to cerebellar folia crus IIA of the Norway rat. *J. Comp. Neurol.*, **302**, 768–778.
- Bower, J.M. & Woolston, D.C. (1983) Congruence of spatial organization of tactile projections to granule cell and Purkinje cell layers of cerebellar hemispheres of the albino rat: vertical organization of cerebellar cortex. *J. Neurophysiol.*, **49**, 745–766.
- Brickley, S.G., Cull-Candy, S.G. & Farrant, M. (1996) Development of a tonic form of synaptic inhibition in rat cerebellar granule cells resulting from persistent activation of GABA<sub>A</sub> receptors. *J. Physiol. (Lond.)*, **497**, 753–759.
- Cohen, D. & Yarom, Y. (1998) Patches of synchronized activity in the cerebellar cortex evoked by mossy-fiber stimulation: questioning the role of parallel fibers. *Proc. Natl Acad. Sci. USA*, **95**, 15032–15036.
- Darian-Smith, I. & Phillips, G. (1964) Secondary neurons within trigemino-cerebellar projection to the anterior lobe of the cerebellum of the cat. *J. Physiol. (Lond.)*, **170**, 53–68.
- Eccles, J.C., Llinás, R.R. & Sasaki, K. (1966a) The excitatory synaptic action of climbing fibres on the Purkinje cells of the cerebellum. *J. Physiol. (Lond.)*, **182**, 268–296.
- Eccles, J.C., Llinás, R.R. & Sasaki, K. (1966b) The mossy fibre-granule cell relay of the cerebellum and its inhibitory control by Golgi cells. *Exp. Brain Res.*, **1**, 82–101.
- Edgley, S.A. & Lidieth, M. (1987) The discharges of cerebellar Golgi cells during locomotion in the cat. *J. Physiol. (Lond.)*, **392**, 315–332.
- Goldberg, J.M. & Fernandez, C. (1971) Physiology of peripheral neurons innervating semicircular canals of the squirrel monkey. III. Variations among units in their discharge properties. *J. Neurophysiol.*, **34**, 676–684.
- Gundappa-Sulur, G., De Schutter, E. & Bower, J.M. (1999) The ascending granule cell axon: an important component of the cerebellar cortical circuitry. *J. Comp. Neurol.*, in press.
- Hartmann, M.J. & Bower, J.M. (1998) Oscillatory activity in the cerebellar hemispheres of unrestrained rats. *J. Neurophysiol.*, **80**, 1598–1604.
- Huerta, M.F., Frankfurter, A. & Harting, J.K. (1983) Studies of the principal sensory and spinal trigeminal nuclei of the rat: projections to the superior colliculus, inferior olive, and cerebellum. *J. Comp. Neurol.*, **220**, 147–167.
- Ito, M. (1984) *The Cerebellum and Neural Control*. Raven Press, New York.
- Jacquin, M.F., Semba, K., Rhoades, R.W. & Egger, M.D. (1982) Trigeminal primary afferents project bilaterally to dorsal horn and ipsilaterally to cerebellum, reticular formation, and cuneate, solitary, supratrigeminal and vagal nuclei. *Brain Res.*, **246**, 285–291.
- Jaeger, D. & Bower, J.M. (1994) Prolonged responses in rat cerebellar Purkinje cells following activation of the granule cell layer: an intracellular *in vitro* and *in vivo* investigation. *Exp. Brain Res.*, **100**, 200–214.
- Llinás, R., Nicholson, C., Freeman, J. & Hillman, D.E. (1968) Dendritic spikes and their inhibition in alligator Purkinje cells. *Science*, **160**, 1132–1135.
- Maex, R. & De Schutter, E. (1998a). The critical synaptic number for rhythmogenesis and synchronization in a network model of the cerebellar granular layer. In Niklasson, L.Bodén, M. & Ziemke, T. (eds.), *International Conference on Artificial Neural Networks*, 98. Springer-Verlag, London, pp. 361–366.
- Maex, R. & De Schutter, E. (1998b) Synchronization of Golgi and granule cell firing in a detailed network model of the cerebellar granule cell layer. *J. Neurophysiol.*, **80**, 2521–2537.
- Marr, D.A. (1969) A theory of cerebellar cortex. *J. Physiol. (Lond.)*, **202**, 437–470.
- Mihailoff, G.A., Kosinski, R.J., Azizi, S.A., Lee, H.S. & Border, B.G. (1992) The expanding role of the basilar pontine nuclei as a source of cerebellar afferents. In Llinás, R.R. & Sotelo, C. (eds.), *The Cerebellum Revisited*. Springer-Verlag, Berlin, pp. 135–164.
- Miles, F.A., Fuller, J.H., Braitman, D.J. & Dow, B.M. (1980) Long-term adaptive changes in primate vestibuloocular reflex. III. Electrophysiological observations in flocculus of normal monkeys. *J. Neurophysiol.*, **43**, 1437–1476.
- Morissette, J. & Bower, J.M. (1996) Contribution of somatosensory cortex to responses in the rat cerebellar cortex granule cell layer following peripheral tactile stimulation. *Exp. Brain Res.*, **109**, 240–250.
- Nicolelis, M.A.L. & Chapin, J.K. (1994) Spatiotemporal structure of somatosensory responses of many-neuron ensembles in the rat ventral posterior medial nucleus of the thalamus. *J. Neurosci.*, **14**, 3511–3532.
- Palay, S.L. & Chan-Palay, V. (1974) *Cerebellar Cortex*. Springer-Verlag, New York.
- Pichitpornchai, C., Rawson, J.A. & Rees, S. (1994) Morphology of parallel fibers in the cerebellar cortex of the rat: an experimental light and electron microscopic study with biocytin. *J. Comp. Neurol.*, **342**, 206–220.
- Rossi, D.J. & Hamann, M. (1998) Spillover-mediated transmission at inhibitory synapses promoted by high affinity alpha6 subunit GABA<sub>A</sub> receptors and glomerular geometry. *Neuron*, **20**, 783–795.
- Schulman, J.A. & Bloom, F.E. (1981) Golgi cells of the cerebellum are inhibited by inferior olive activity. *Brain Res.*, **210**, 350–355.
- Shambes, G.M., Gibson, J.M. & Welker, W. (1978) Fractured somatopy in granule cell tactile areas of rat cerebellar hemispheres revealed by micromapping. *Brain Behav. Evol.*, **15**, 94–140.
- Sharp, F.R.M.F.G., Morgan, C.W., Morton, M.T. & Sharp, J.W. (1988) Common fur and mystacial vibrissae parallel sensory pathways: 14C2-deoxyglucose and WGA-HRP studies in the rat. *J. Comp. Neurol.*, **270**, 446–469.
- Thach, W.T. (1967) Somatosensory receptive fields of single units in cat cerebellar cortex. *J. Neurophysiol.*, **30**, 675–696.
- Van Kan, P.L.E., Gibson, A.R. & Houk, J.C. (1993) Movement-related inputs to intermediate cerebellum of the monkey. *J. Neurophysiol.*, **69**, 74–94.
- Vos, B.P., Volny-Luraghi, A., Maex, R. & De Schutter, E. (1999) Parallel fibres synchronize synchronous activity in cerebellar Golgi cells. *J. Neurosci.*, **19**(RC6), 1–5.
- Vranesic, I., Iijima, T., Ichikawa, M., Matsumoto, G. & Knöpfel, T. (1994) Signal transmission in the parallel fiber Purkinje cell system visualized by high-resolution imaging. *Proc. Natl Acad. Sci. USA*, **91**, 13014–13017.
- Waite, P.M.E. & Tracey, D.J. (1995) Trigeminal sensory system. In Paxinos, G. (ed.), *The Rat Nervous System*, (2nd edn.) Academic Press Inc, San Diego, pp. 705–724.
- Wall, M.J. & Usowicz, M.M. (1997) Development of action potential-dependent and independent spontaneous GABA<sub>A</sub> receptor-mediated currents in granule cells of postnatal rat cerebellum. *Eur. J. Neurosci.*, **9**, 533–548.
- Watanabe, D., Inokawa, H., Hashimoto, K., Suzuki, N., Kano, M., Shigemoto, R., Hirano, T., Toyama, K., Kaneko, S., Yokoi, M., Moriyoshi, K., Suzuki, M., Kobayashi, K., Nagatsu, T., Kreitman, R.J., Pastan, I. & Nakanishi, S. (1998) Ablation of cerebellar Golgi cells disrupts synaptic integration involving GABA inhibition and NMDA receptor activation in motor coordination. *Cell*, **95**, 17–27.
- Watson, C.R.R. & Switzer, R.C. III (1978) Trigeminal projections to cerebellar tactile areas in the rat: origin from n. interpolaris and n. principalis. *Neurosci. Lett.*, **10**, 77–82.
- Welker, W. (1987) Spatial organization of somatosensory projections to granule cell cerebellar cortex: Functional and connectional implications of fractured somatopy (summary of Wisconsin studies). In King, J.S. (ed.), *New Concepts in Cerebellar Neurobiology*. Alan R. Liss, Inc., New York, pp. 239–280.
- Woolston, D.C., La Londe, J.R. & Gibson, J.M. (1982) Comparison of response properties of cerebellar and thalamic-projecting interopolaris neurons. *J. Neurophysiol.*, **48**, 160–173.